ISSN (Print) : 0974-6846
Indian Journal of Science and Technology, Vol 9(42), DOI: 10.17485/ijst/2016/v9i42/101980, November 2016 ISSN (Online) : 0974-5645

Mechanical Properties and Phase Transformations in Resistance Spot Welded Dissimilar Joints of AISI409M/AISI301 Steel

A. Subrammanian[1*], D. B. Jabaraj[2], J. Jayaprakash[3] and V. K. Bupesh Raja[4]

[1]Department of Mechanical Engineering, St Peters University, Avadi, Chennai - 600054, Tamil Nadu, India; prakash221271@gmail.com

[2]Dr MGR Educational and Research Institute University, Chennai - 600095, Tamil Nadu, India; jabaraj2009@yahoo.com

[3]Department of Mechanical Engineering, Dr MGR Educational and Research Institute University, Chennai - 600095, Tamil Nadu, India; profjaya@gmail.com

[4]Department of Automobile Engineering, Sathyabama University, Chennai - 600119, Tamil Nadu, India; bupeshvk@gmail.com

Abstract

Objectives: This study aims to investigate the mechanical properties and phase transformations in dissimilar metal joints between AISI 301 Austenitic Stainless Steel and AISI 409M Ferritic Stainless Steel, joined by resistance spot welding. **Methods/Analysis:** Mechanical properties such as tensile shear strength, failure energy, failure mode, nugget size and surface indentation were analysed at varying current ratings. Macrostructure was examined for size and shape. Microstructure at various locations such as, fusion zone and heat affected zones were investigated. Micro hardness measurement was done at various locations along the weld. **Findings:** Peak load incremented progressively with rise in welding current, till the commencement of severe expulsion. Weld zone hardness showed a higher value than that of nearby heat affected zones and parent metals. Increment in welding current resulted in enlargement of weld nugget and rise in energy absorption capacity. Electrode indentation values were seen to be correlated with welding current values positively. Fusion zone microstructure consists of marten site and ferrite. Asymmetrical nugget shape was observed. **Novelty/Improvement:** This study explores the properties**,** both mechanical and microstructure of AISI 409M-AISI 301 steel dissimilar joint, joined by resistance spot welding.

Keywords: AISI301, AISI409M, Failure mode, Microstructure, Peak load

1. Introduction

Resistance Spot Welding (RSW) is a prominent metal joining process[1]. Both electric current and mechanical pressure are applied together to make joints in RSW process[2]. RSW is an attractive choice for automobile and rail car manufacturing industries as it is less expensive, faster and can be automated easily. The joint formation in RSW is influenced by various input variables like welding current, welding time and electrode force[3].

Ferritic Stainless Steels (FSS) are considered as one of the important type of stainless steels and are also considered as less expensive substitutes for austenitic stainless steels[4]. Nowadays, Ferritic Stainless Steel finds many applications in automobile and rail car manufacturing. Austenitic Stainless Steel (ASS) is a preferred choice in rail car manufacturing for structural applications[6].

Dissimilar metal welding is commonly used in industries nowadays. The quality of such joints will often be vital to the proper functioning of the whole unit. Many

*Author for correspondence

research works[7,8] have been reported in the past on dissimilar metal spot welding. Many studies have been reported on dissimilar spot welding between Austenitic Stainless Steel and various low carbon steels. However studies reported on spot welding between ASS and FSS are limited. Such joints find application in railcar manufacturing industries. A deep understanding about the effect of RSW on the mechanical behaviour of the weld is essential to improve the performance of the joint. Hence, in this work, an effort is made to investigate the mechanical characteristics and phase transformations of dissimilar joints between AISI301 and AISI409M joined with spot welding.

2. Materials and Methods

2.1 Material

In this work, specimens of Ferritic Stainless Steel AISI 409M and Austenitic Stainless Steel AISI301 were welded by RSW. Sheet thickness for both the materials was 2 mm. Test samples for tensile shear test were made ready, confirming to ISO 14273 standards. The dimensions of the test coupon taken for the current work were 60 mm width wise and 138 mm length wise. Chemical composition was measured for both the materials with the help of a spectrometer and the same is shown in Table 1.

2.2 Experimental

The experiment was conducted on a resistance spot welder (make-Jaya Hind Sciaky, model- P252, 75 KVA). RWMA class 3 electrodes with tip diameter 8 mm were used for welding. Welding was done with different welding current values from 7 kA (kilo Ampere) to 14 kA, with a regular addition of 1 kA. Meanwhile other parameters like electrode force and weld time were kept constants, at 4 kN (Kilo Newton) and 15 cycles (1 cycle = 20 milliseconds) respectively, based on preliminary trials. Also squeeze time, holding time and off time were chosen as 40 cycles, 20 cycles and 20 cycles respectively.

2.2.1 Mechanical Tests

Peak load during failure was measured on a Universal Tensile Testing Machine (UTM). Peak load, corresponding to the highest point in the load-elongation curve of tensile shear test, was recorded for each test specimen. The energy absorbed during failure was determined by calculating the area below the load-elongation curve, up to the point of maximum load, of tensile shear test. Mode of failure such as, interfacial mode or pull out mode, in each sample was noted after the shear test. Peel test was carried out on specimens, welded at varying currents and average diameter of the nugget was recorded, corresponding to each current value. Indentation, the depression made by the electrode tip on the surface of the sheet, was recorded for each specimen, using a digital depth gauge with an accuracy of 0.01 mm to analyse the effect of current on it.

2.2.2 Metallurgical Study

Specimens for microstructure examination were prepared. Etching of the specimens was done with Kalling's No. 1 etchant. Microstructure examination was carried out at various locations in the cross section of the weld by optical microscopy. Fusion zone size was also measured through microscope using wire cross sections.

Hardness tester, make-Shimadzu, 0.5 Kg was employed to make micro hardness measurement at various locations across the weld. Hardness was recorded at base metal region of FSS (BM FSS), low/high temperature heat affected zone (LTHAZ /HTHAZ) of FSS, Fusion Zone (FZ), Heat Affected Zone of ASS (HAZ ASS) and Base Metal region of ASS (BM ASS).

2.2.3. Macroscopic Test

Macrograph of spot weld was examined to assess the geometrical characteristics of the weld such as size and shape of the nugget, amount of penetration at the fusion zone etc.

Table 1. Chemical composition of test materials (percentage by weight)

Grade	C	Si	Mn	P	S	Cr	Cu	Ni	Ti	Al	Fe
AISI 409M	0.030	0.418	0.879	0.028	0.013	12.33	0.014	0.071	0.02	0.014	Balance
AISI 301	0.068	0.693	1.520	0.011	0.018	16.09	0.225	6.009	----	----	Balance

3. Results and Discussion

3.1 Mechanical Properties

Various output parameters such as peak load (tensile shear strength), failure energy and nugget size were measured to investigate the mechanical behaviour of the weld joint. A positive correlation was noticed between peak load and current ratings. Scatter plot of peak load with current is shown in Figure 1. However, it can be seen from the graph that at higher current values, tensile shear strength does not increase with further increase in current due to expulsion. Expulsion results in heat and metal loss from the weld, causing reduction in peak load. Fusion zone size increases with increase in current value, due to more heat input and subsequent increased melting of metal. The correlation between nugget diameter and current is given in Figure 2. As in the case of peak load, nugget diameter ceases to be in direct relationship with welding current values, at high current ratings, due to excessive expulsion. It is well documented in studies in the past, that nugget size holds the largest influence in controlling the peakload[9,10].

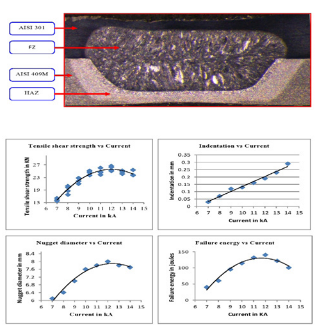

Figure 1. Tensile shear strength-current graph.

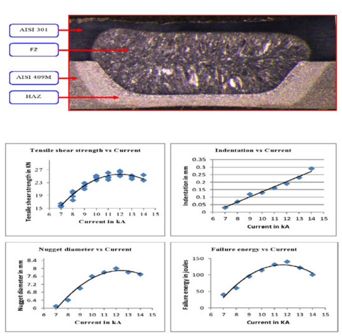

Figure 2. Nugget diameter-current graph.

Failure energy or the energy absorbing capacity of the weld joint was seen improving with progressive increment in welding current values as shown in Figure 3. Failure energy in a tensile shear test depends upon the maximum load and the elongation during failure. The failure energy or energy absorption capacity of the joint increases with increase in current rating, primarily due to increase in fusion zone size. Again it can be noticed that expulsion associated with high welding current results in drop of failure energy.

In spot welding, usually there are two modes of failure such as interfacial mode and pull out mode. In interfacial mode, failure occurs when a crack develops and moves along a plane parallel to the surface of the specimen sheet, whereas, in pull out type of failure, the nugget comes out wholly from one of the sheets in the form of a button[11,12]. In the current work, it was observed that the samples welded with a current rating of 10 kA and above underwent pullout mode of fracture.

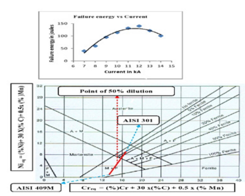

Figure 3. Failure energy-current graph.

Pullout mode of failure is usually preferred over interfacial mode due to the higher tensile shear strength and failure energy associated with the former[12]. Interestingly the failure location in all the samples with pullout mode of failure was at the ASS side, though tensile strength of ASS is more than that of FSS. The HAZ width of ASS was significantly less than that of FSS. Even though, the fusion zone area of ASS is larger than that of FSS, the perimeter of the circle containing both FZ and HAZ in case of ASS is significantly less than that of FSS. As a result, there is a large area of cross section along the thickness of FSS to resist the external load compared to that of ASS. Therefore, during tensile test, fracture occurred in the ASS base metal.

Indentation values were analysed in relation with the current values. Correlation between indentation and current is given in Figure 4.

Increased amount of indentation was noticed with increasing current values. Indentation results in poor surface finish and therefore is not desirable. Higher heat input subsequent to increased current rating promotes plastic deformation at the surface of the sheet, where electrode force is acting. This leads to deeper indentation on the surface of the nugget.

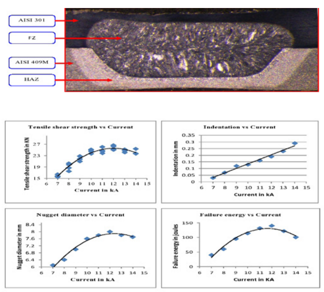

Figure 4. Indentation-current graph.

3.2 Macrograph

The macroscopic image of the spot welded joint is given in Figure 5. An asymmetrical nugget shape has been observed, in dissimilar spot welded FSS/ASS joint, with the size of the FZ on ASS side, larger than the other side. There are differences in thermal and electrical properties of ASS and FSS. The irregular shape of the nugget can be attributed to the same.

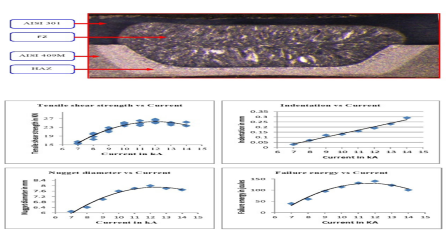

Figure 5. Macrograph of the weld.

3.3 Microstructure

A fully ferritic microstructure was seen in the base metal of FSS (figure 6). In case of ASS base metal, austenite microstructure was noticed (figure 7).

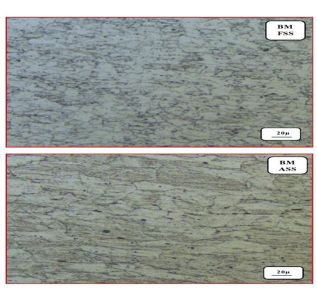

Figure 6. BM FSS microstructure.

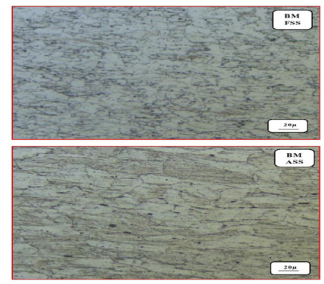

Figure 7. BM ASS microstructure.

In the HAZ of FSS, while examining the microstructure, two distinct regions were observed (figure 8). The region close to the base metal, where relatively lower temperature prevailed (LTHAZ), consisted of fine grains of ferrite whereas the region next to it and close to the fusion zone, where relatively higher temperature prevailed during welding (HTHAZ) consisted of coarse grains of ferrite[13].

As per the Fe-Cr-C pseudo-binary phase diagram[14] for low chromium Ferritic Stainless Steel (13% Cr), at elevated temperature below melting point, the ferrite microstructure at room temperature changes to either austenite+ delta ferrite or delta ferrite alone as represented by the line drawn through 0.03% in X axis Figure 9. Here the LTHAZ and HTHAZ represent the delta ferrite+austenite ($\delta + \gamma$) and delta ferrite (δ) phase respectively. In the LTHAZ, under elevated temperature, some austenite is formed around the grain boundaries which prevent grain growth in this region. During rapid cooling, that is usually associated with RSW; the same austenite is transformed to martensite and results in increased hardness. In HTHAZ region, at elevated temperature, delta ferrite is formed. However, due to rapid cooling, austenite formation is suppressed and hence the resultant microstructure is fully ferritic with a fair amount of grain growth. Lower value of micro hardness at this region is in good agreement with its coarse grain ferrite microstructure.

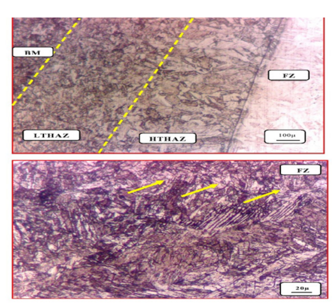

Figure 8. HAZ FSS microstructure.

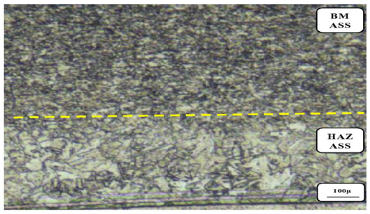

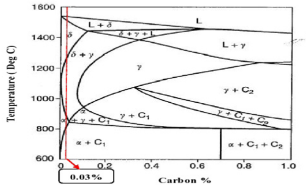

Figure 9. Fe-Cr-C pseudo-binary phase diagram for low chromium Ferritic Stainless Steel (13% Cr).

Austenitic microstructure was found in the HAZ of ASS. Though some amount of grain growth could be seen, it was not as large as FSS (figure 10).

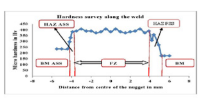

Figure 10. HAZ ASS microstructure.

Microstructure of fusion zone was found to be consisting predominantly of martensite and ferrite (figure 11). Microstructure of fusion zone in dissimilar metal welding can be predicted with the help of Schaeffler diagram. At 50% diffusion, the resultant fusion zone microstructure in the Schaeffler diagram indicates a combination of ferrite and martensite (figure 12). The reason for obtaining higher micro hardness values at fusion zone can be related to the formation of martensite.

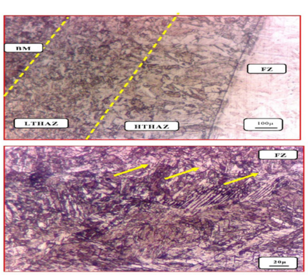

Figure 11. FZ Microstructure, arrow marks shows martensite.

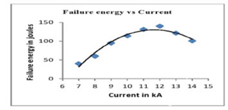

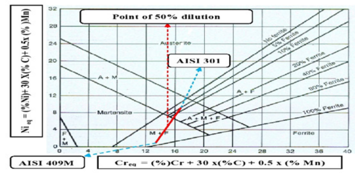

Figure 12. Schaeffler diagram to predict the FZ microstructure.

3.4 Micro Hardness

Micro hardness measurement was carried out across the weld at different locations and the values were as shown in Figure 13. Hardening of the weld zone was noticed compared to base metal and HAZ. This can be related to the formation of martensite in the weld zone. Along the HAZ of FSS, micro hardness first increased sharply through the LTHAZ to a maximum and then decreased to a minimum level in the HTHAZ. In the LTHAZ of FSS, increasing hardness is mainly due to grain refinement and it steadily increases with the maximum temperature prevailed during the welding. In the HTHAZ, lower values of micro hardness were observed due to grain growth. The high cooling rate associated with RSW inhibits the transformation of high temperature delta ferrite to austenite and hence transform directly to ferrite with larger grains. On the other hand, micro hardness increased steadily along the HAZ of ASS from base metal to fusion zone boundary. Ratio of average fusion zone hardness to FSS base metal hardness was found to be 2.18 approximately and that for ASS base metal was found to be 1.63.

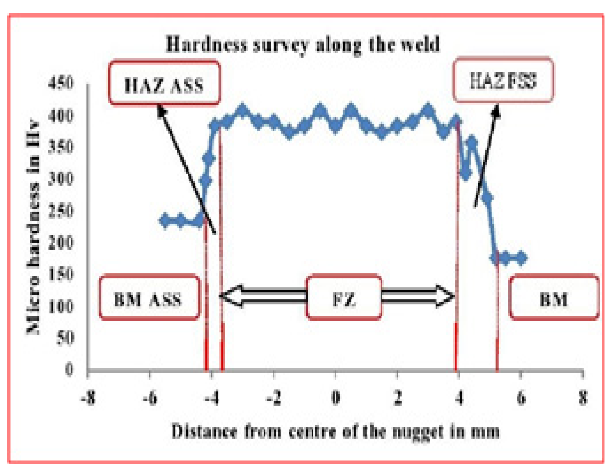

Figure 13. Micro hardness profile of the weld.

4. Conclusions

Weld zone hardness was higher with respect to base metals and heat affected zones. Positive variations were noticed in nugget diameter and failure energy with respect to increasing welding current values. Electrode indentation on the nugget surface increased with higher current values. Fusion zone microstructure consists of martensite and ferrite. Asymmetrical nugget shape was observed with Austenitic Stainless Steel side being larger than Ferritic Stainless Steel side. Grain coarsening was noticed at the high temperature HAZ region.

5. Acknowledgement

Authors are grateful to Advanced Welding Training Institute (AWTI), Integral Coach Factory, Indian Railways, Chennai, India, for extending facilities of Chemical and Metallurgical Testing Laboratory, to carry out this investigation.

6. References

1. Shamsul JB, Hisyam MM. Study of spot welding of Austenitic Stainless Steel type 304. Journal of Applied Sciences Research. 2007 Jan; 3(11):1494–7.
2. Pouranvari M. Effect of welding current on the mechanical response of resistance spot welds of unequal thickness steel sheets in tensile-shear loading condition. International Journal of Multidisciplinary Sciences and Engineering. 2011 Sep; 5(12):63–7.
3. Hamidinejad SM, Kolahan F, Kokabi AH. The modeling and process analysis of Resistance Spot Welding on galvanized steel sheets used in car body manufacturing. Materials and Design. 2012; 34:759–67.
4. Feng JC, Wang YR, Zhang ZD. Nugget growth characteristic for AZ31B magnesium alloy during resistance spot welding. Science and Technology of Welding and Joining. 2006; 11(2):154–62.
5. Pouranvari M, Marashi SPH, Alizadehsh M. Welding metallurgy of dissimilar AISI 430/DQSK steels resistance spot welds. Welding Journal. 2015 Jun; 94(6):203–10.
6. Pouranvari M, Ranjbarnoodeh M. Effect of welding current on energy absorption of AISI 304 Resistance Spot Welds. Research Journal of Applied Sciences Engineering and Technology. 2012 Sep; 4(17):2911–4.
7. Alenius M, Somervuori, Hannien H. Exploring the mechanical properties of spot welded dissimilar joints for stainless and galvanized steels. Welding Journal. 2006 Dec; 85(12):305–13.
8. Marashi P, Pouranvari M, Amirabdollahian S, Abedi A, Goodarzi M. Microstructure and failure behavior of dissimilar resistance spot welds between low carbon galvanized and Austenitic Stainless Steels. Materials Science and Engineering A. 2008 May; 480(1-2):175–80.
9. Pouranvari M. Analysis of fracture mode of galvanized low carbon steel resistance spot welds. International Journal of Multidisciplinary Sciences and Engineering. 2011 Sep; 2(6):36–40.
10. Pouranvari M, Ranjbarnoodeh E. Resistance Spot Welding characteristic of ferrite-martensite DP600 dual phase advanced high strength steel-part III: Mechanical properties. World Applied Sciences Journal. 2011 Jan; 15(11):1521–6.
11. Sun X, Stephens EV, Khaleel MA. Effects of fusion zone size and failure mode on peak load and energy absorption of advanced high strength steel spot welds under lap shear loading conditions. Engineering Failure Analysis. 2008 Jun; 15(4):356–67.
12. Pouranvari M, Asgari HR, Mosavizadeh SM, Marashi PH, Goodarzi M. Effect of weld nugget size on overload failure mode of resistance spot welds. Science and Technology of Welding and Joining. 2007; 12(3):217–25.
13. Subrammanian A, Jabaraj DB, Bupesh Raja VK. Microstructure and mechanical properties of resistance spot welded joints of AISI 409M Ferritic Stainless Steel. Transactions of Indian Institute of Metals. 2016; 69(3):767–74.
14. Lippold JC, Kotecki J. Welding metallurgy and weldability of stainless steels. John Wiley and Sons; 2011.